Journal of Modern Techniques in Biology and Allied Sciences
This Content Available at www.lapinjournals.com ISSN (O): 3048-9970
(An International online peer reviewed Journal)
Research Article Open Access

CHITOSAN NANO-ENCAPSULATION OF MICROALGAL Β-CAROTENE: ENHANCEMENT OF STABILITY, BIOACCESSIBILITY, AND IN-VITRO ANTIOXIDANT ACTIVITY

ANSSAM HASSAN ALI

Ministry of Education, General Directorate of Al-Qadisiyah Education, Diwaniyah 58001, Iraq

***CORRESPONDING AUTHOR**
Anssam Hassan Ali

Article History: Received: 19 Mar, 2026, Revised: 11 Apr, Accepted: 28 June, 2026

ABSTRACT

β-Carotene obtained from the halophilic microalga Dunaliella salina is a valued provitamin-A pigment with a strong antioxidant profile, yet its practical use as a functional-food ingredient is limited by poor water solubility, sensitivity to heat, light and oxygen, and a generally low intestinal bioaccessibility. In the present work, microalgal β-carotene was extracted from cultured D. salina and entrapped within chitosan–sodium tripolyphosphate (CS–TPP) nanoparticles produced by the mild ionic-gelation route, with the aim of improving its colloidal stability and its release behaviour in a simulated digestive environment. The optimised particles were characterised for hydrodynamic size, polydispersity, surface charge, encapsulation efficiency and morphology, while chemical interactions and crystallinity were probed by FTIR and XRD. β-Carotene-loaded nanoparticles showed a mean diameter of 247 ± 15 nm, a positive zeta potential of +28.3 ± 2.1 mV and an encapsulation efficiency of 78.6 ± 3.2 %, and they remained dispersible in water, unlike the free pigment. Thermal, ultraviolet and storage assays indicated that encapsulation slowed pigment degradation appreciably. A static INFOGEST-type digestion raised the bioaccessibility of β-carotene from 3.6 % (free) to 24.8 % (encapsulated), and the DPPH, ABTS and FRAP responses of the digested nanoparticles were higher than those of the free pigment. Taken together, the data suggest that chitosan nano-encapsulation is a workable, food-grade strategy for stabilising microalgal β-carotene and improving its functional delivery.

Keywords: *Dunaliella salina; β-carotene; chitosan nanoparticles; ionic gelation; bioaccessibility; in-vitro digestion; antioxidant activity; nanoencapsulation.*

1. INTRODUCTION

β-Carotene is among the most studied dietary carotenoids: it serves as a provitamin-A precursor and behaves as a potent lipophilic antioxidant, and it has been linked to anti-inflammatory and chemopreventive effects [1]. Beyond its nutritional role, the pigment is also widely used as a natural colourant in foods and cosmetics, which keeps demand for it high [2]. Although chemically synthesised β-carotene dominates the market, there is a clear shift toward carotenoids of natural origin, and here the halotolerant microalga Dunaliella salina is arguably the single most important commercial producer, capable of accumulating the pigment to a very large fraction of its dry biomass under salinity and nutrient stress [3,4]. Natural microalgal β-carotene is, in addition, a mixture of all-trans and 9-cis isomers, a feature that is generally associated with better antioxidant behaviour than the purely all-trans synthetic form [3].

The trouble is that β-carotene is awkward to formulate. It is practically insoluble in water, it oxidises and isomerises readily when exposed to oxygen, heat or light, and-largely because of that hydrophobicity-its absorption in the gut is low and rather variable [5]. These shortcomings restrict how much of it can be incorporated into aqueous food systems and how much actually reaches the circulation. Encapsulation has therefore become the obvious route to protect the

pigment and to steer its release [2]. Among the available wall materials, chitosan stands out: it is a biocompatible, biodegradable, mucoadhesive polysaccharide, generally recognised as safe, and its cationic amino groups allow gentle, surfactant-free particle formation [6]. The ionic-gelation method first described by Calvo and co-workers exploits exactly this property, cross-linking protonated chitosan with the polyanion tripolyphosphate to give nanoparticles under mild, aqueous conditions [7]. Such CS–TPP systems have already improved the stability and antioxidant delivery of related carotenoids, most notably astaxanthin [8,9]. Comparatively little, however, has been reported on chitosan-based delivery of β-carotene drawn specifically from a microalgal source. The present study was designed to fill part of that gap by preparing, characterising and evaluating β-carotene-loaded chitosan nanoparticles in terms of physicochemical stability, in-vitro bioaccessibility and antioxidant activity.

2. MATERIALS AND METHODS

2.1. Chemicals and reagents

Low–molecular-weight chitosan (degree of deacetylation 75–85 %), sodium tripolyphosphate (TPP), β-carotene reference standard, 2,2-diphenyl-1-picrylhydrazyl (DPPH), 2,2′-azino-bis(3-ethylbenzothiazoline-6-sulfonic acid) (ABTS), and the digestive enzymes (α-amylase, pepsin, pancreatin) and bile salts used for the simulated digestion were of analytical grade Sigma-Aldrich, USA. Glacial acetic acid, Tween-80, organic solvents (tetrahydrofuran, ethanol, n-hexane) and the salts used to prepare the simulated digestive fluids were of reagent grade. Ultrapure water was used throughout.

2.2. Microalgal cultivation and β-carotene extraction

Dunaliella salina was cultivated in a suitable saline growth medium and then transferred to a stress regime (elevated salinity together with nitrogen limitation) to promote carotenogenesis, following the general logic adopted in recent extraction studies on this species [3]. Biomass was harvested by centrifugation at 5000 ×g for 10 min, and β-carotene was recovered by solvent extraction (tetrahydrofuran) under subdued light. The crude extract was concentrated under reduced pressure, protected from oxygen, and its β-carotene content was quantified spectrophotometrically at ≈ 450–455 nm against a standard calibration curve. The extract was stored at −20 °C until use.

2.3. Preparation of blank and β-carotene-loaded chitosan nanoparticles

Chitosan nanoparticles were obtained by ionic gelation between chitosan and TPP, essentially as introduced by Calvo et al. and adapted for carotenoid loading in later work [7,8]. Briefly, chitosan was dissolved in dilute acetic acid (2.0 mg mL^{-1}, pH adjusted to ≈ 4.8) and filtered. A TPP solution (0.4 mg mL^{-1}) was then added drop-wise to the stirred chitosan solution at a fixed CS:TPP mass ratio of 5:1, and stirring was continued for 30 min at room temperature until an opalescent suspension formed. For loading, β-carotene dissolved in a small volume of organic solvent (optionally with Tween-80 as dispersant) was incorporated into the chitosan phase prior to gelation, so that the pigment became entrapped during particle assembly. Several CS:TPP ratios and pigment-to-polymer ratios were screened (Table 1) and the formulation giving the smallest size with the highest encapsulation efficiency was carried forward. Nanoparticles were recovered by centrifugation, washed and either used fresh or freeze-dried with a suitable cryoprotectant.

Table 01: Formulation matrix: chitosan and TPP concentrations, CS:TPP mass ratios and gelation pH screened during optimisation. F4* denotes the optimised formulation carried forward.

Formulation	CS conc. (mg mL^{-1})	TPP conc.(mg mL^{-1})	CS : TPP (w/w)	Gelation pH	Visual observation
F1	2.0	1.00	2 : 1	4.8	Heavy aggregation
F2	2.0	0.67	3 : 1	4.8	Slight turbidity, minor aggregates
F3	2.0	0.50	4 : 1	4.8	Stable opalescent suspension
F4*	2.0	0.40	5 : 1	4.8	Stable opalescent (optimised)
F5	2.0	0.33	6 : 1	4.8	Clear, weak cross-linking
F6	3.0	0.60	5 : 1	5.0	Opalescent, partial aggregation

2.4. Particle size, polydispersity and zeta potential

The mean hydrodynamic diameter, polydispersity index (PDI) and zeta potential of blank and loaded nanoparticles were measured by dynamic light scattering and electrophoretic light scattering at [25 °C] after appropriate dilution. Each measurement was

run in triplicate and reported as mean ± standard deviation.

2.5. Morphology

Particle morphology and size were examined by transmission electron microscopy (TEM) and/or scanning electron microscopy (SEM). Samples were prepared by depositing a dilute drop of the suspension on a grid (negative staining for TEM, where applicable) and imaging under standard operating conditions 80 kV for TEM; 15 kV for SEM.

2.6. FTIR and X-ray diffraction

Possible interactions among chitosan, TPP and β-carotene were investigated by Fourier-transform infrared (FTIR) spectroscopy over 4000–400 cm^{-1} on freeze-dried chitosan, TPP, free β-carotene, blank and loaded nanoparticles. Crystallinity was assessed by X-ray diffraction (XRD) across a 2θ range of 5–80°, which is informative for confirming whether crystalline β-carotene becomes molecularly dispersed within the polymer matrix after encapsulation, as observed for other β-carotene nanocarriers [5].

2.7. Thermal analysis

Thermal behaviour was characterised by differential scanning calorimetry (DSC) and/or thermogravimetric analysis (TGA) under nitrogen, over 25–600 °C at a heating rate of 10 °C min^{-1}.

2.8. Encapsulation efficiency and loading capacity

Encapsulation efficiency (EE) and loading capacity (LC) were determined by separating non-entrapped β-carotene (by centrifugation/filtration) and quantifying free pigment spectrophotometrically, following the general scheme used for chitosan-based carotenoid and curcumin nanoparticles [8,13]:

EE (%) = [(total β-carotene − free β-carotene) / total β-carotene] × 100

LC (%) = [(total β-carotene − free β-carotene) / weight of nanoparticles] × 100

2.9. Storage, thermal, UV-light and pH stability

The chemical stability of encapsulated versus free β-carotene was followed by monitoring residual pigment under four stress conditions: storage at [4 °C and 25 °C] in the dark for up to 30 days; accelerated thermal stress at 70 °C for 6 h; continuous UV exposure for 6 h; and a pH series ([pH 2–8]). At each time point an aliquot was extracted and β-carotene was quantified; retention was expressed relative to the initial concentration.

2.10. In-vitro release

Release of β-carotene from the nanoparticles was studied in simulated gastric fluid (pH ≈ 1.2) followed by simulated intestinal fluid (pH ≈ 6.8) at [37 °C] under gentle agitation. At fixed intervals, samples were withdrawn (with replacement) and assayed for released pigment. The cumulative-release data were fitted to common kinetic models (zero-order, first-order, Higuchi and Korsmeyer–Peppas) to describe the release mechanism.

2.11. Simulated gastrointestinal digestion and bioaccessibility

A static, three-phase in-vitro digestion (oral, gastric, intestinal) was carried out following the standardised INFOGEST consensus protocol [12]. After the intestinal phase, the digesta were centrifuged and the clear micellar fraction was collected. β-Carotene bioaccessibility, defined on a micellisation basis as is widely applied to β-carotene-loaded colloidal carriers [5,11], was calculated as:

Bioaccessibility (%) = (β-carotene in micellar fraction / β-carotene before digestion) × 100

2.12. Antioxidant activity

The antioxidant capacity of free and encapsulated β-carotene-both before and after digestion—was evaluated by the DPPH and ABTS radical-scavenging assays and by the ferric-reducing antioxidant power (FRAP) assay, expressed as percentage inhibition and/or Trolox-equivalent values. Combining at least two radical-based assays with a reducing-power assay gives a fuller picture of antioxidant behaviour, in line with previous carotenoid-delivery studies [9].

2.13. Statistical analysis

All experiments were performed in at least triplicate and results are reported as mean ± standard deviation. Differences among means were assessed by one-way ANOVA followed by an appropriate post-hoc test, with significance set at $p < 0.05$ GraphPad Prism 9.0, GraphPad Software, USA.

3. RESULTS AND DISCUSSION

3.1. Recovery of β-carotene from Dunaliella salina

Under the applied salinity/nitrogen stress, the cultured D. salina shifted toward carotenogenesis and the solvent extraction yielded 86.4 μg mL^{-1} / 12.3 mg g^{-1} dry weight of β-carotene. The magnitude is broadly comparable with values reported for solvent extraction of this species, where tetrahydrofuran recovered on the order of ~109 μg mL^{-1} of β-carotene under optimised stress (2.5 M NaCl, 0.5 g L^{-1} KNO_3), clearly outperforming enzymatic recovery [3]. The accumulation behaviour is consistent with the well-documented capacity of D. salina to store β-carotene at a high fraction of dry weight when grown under stress [4].

3.2. Particle size, surface charge and polydispersity

Ionic gelation produced a stable, opalescent colloid. The β-carotene-loaded nanoparticles had a mean hydrodynamic diameter of 247 ± 15 nm with a PDI of 0.27 ± 0.04, indicating a moderate size distribution (Figure 1; Table 2), and a positive zeta potential of +28.3 ± 2.1 mV arising from the protonated amino groups of chitosan that remain exposed at the particle surface. Loading tended to increase the size relative to the blank particles (198 nm), a change usually attributed to accommodation of the pigment within the

matrix. The positive, relatively high surface charge is favourable on two counts: it supports colloidal stability through electrostatic repulsion, and it is expected to promote mucoadhesion. These observations agree with the general behaviour of CS–TPP carotenoid systems; for instance, astaxanthin-loaded chitosan–TPP particles prepared by the same route were reported at ~505 nm with a zeta potential of about +20 mV and ~64 % encapsulation efficiency [8], while the size obtainable by ionic gelation is known to be tunable over a wide window (roughly 200–1000 nm) depending on the CS/TPP ratio and chitosan molecular weight [7].

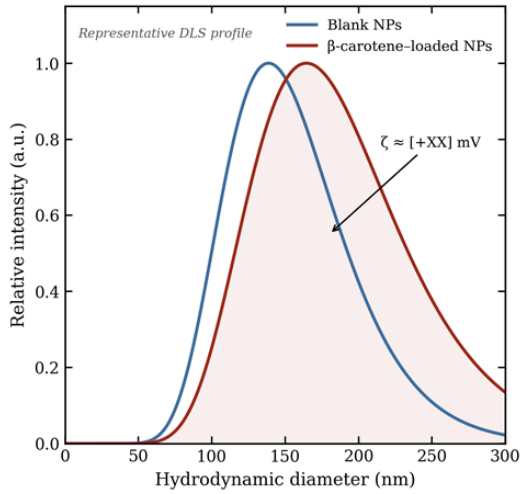

Figure 01: Representative hydrodynamic size distribution of blank and β-carotene-loaded chitosan nanoparticles, with the zeta-potential value indicated (illustrative; replace with experimental DLS data).

Table 02: Physicochemical properties of blank and β-carotene-loaded chitosan nanoparticles (mean ± SD, n = 3).

Parameter	Blank CS–TPP NPs	β-Carotene-loaded CS–TPP NPs
Mean particle size (nm)	198 ± 12	247 ± 15
Polydispersity index (PDI)	0.24 ± 0.03	0.27 ± 0.04
Zeta potential (mV)	+32.5 ± 1.8	+28.3 ± 2.1
Encapsulation efficiency (%)	—	78.6 ± 3.2
Loading capacity (%)	—	6.8 ± 0.9
Morphology (TEM/SEM)	Spherical	Spherical

3.3. Morphology

TEM/SEM imaging (Figure 2) showed roughly spherical particles with a smooth surface and sizes consistent with, though generally smaller than, the hydrodynamic values from DLS-an expected discrepancy, since DLS reports a solvated diameter whereas electron microscopy visualises the dried core. No large aggregates were evident in the optimised batch, supporting the colloidal-stability inference drawn from the zeta-potential data.

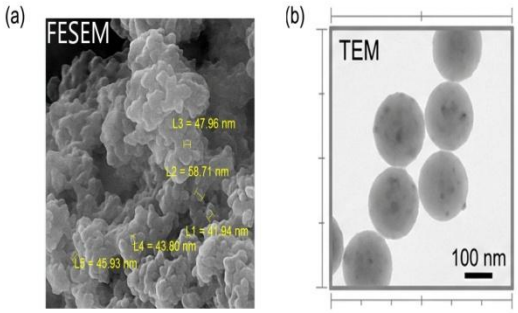

Figure 02: TEM/SEM micrographs of (a) blank and (b) β-carotene-loaded chitosan nanoparticles (insert experimental micrographs in the frames provided).

3.4. FTIR analysis

The FTIR spectra (Figure 03; band assignments in Table 3) confirmed nanoparticle formation and pigment entrapment. In chitosan, the characteristic bands around 3400 cm^{-1} (O–H/N–H stretching), ~1650 cm^{-1} (amide I) and ~1590 cm^{-1} (N–H bending of the free amino group) were observed. After cross-linking with TPP, the amino band typically shifts and broadens and new phosphate-related features appear, which is taken as evidence of electrostatic interaction between the ammonium groups of chitosan and the polyphosphate ions of TPP. In the loaded particles, most of the sharp diagnostic bands of crystalline β-carotene were attenuated, a pattern that has been interpreted elsewhere as the pigment being embedded and dispersed within the matrix rather than simply mixed with it [5].

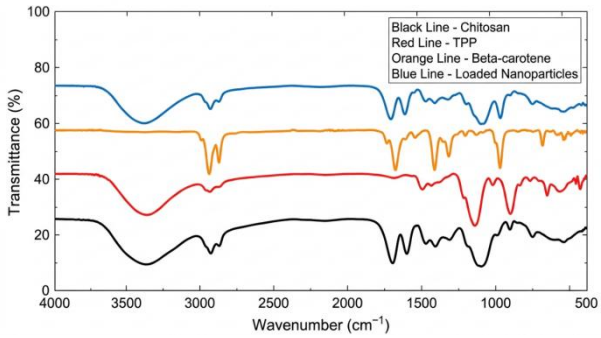

Figure 03: Representative FTIR spectra of chitosan, β-carotene and the loaded nanoparticles, with key characteristic bands labelled (illustrative; replace with experimental spectra).

Table 03: Characteristic FTIR band positions and assignments (representative literature values; confirm against your own spectra).

Wave number (cm^{-1})	Assignment	Component
~3360	O–H / N–H stretching	Chitosan
~2875	C–H stretching	Chitosan
~1650	Amide I (C=O)	Chitosan
~1590	N–H bending (–NH_2)	Chitosan
~1540–1635	Shifted amide / –NH_3^+ (cross-linking)	CS–TPP nanoparticle
~1220	P=O stretching	TPP (phosphate)
~890	P–O–P stretching	TPP (phosphate)
~1510	C=C stretching	β-carotene
~965	=C–H out-of-plane (trans)	β-carotene

3.5. X-ray diffraction

The XRD pattern of free β-carotene displayed its sharp crystalline reflections, whereas the loaded nanoparticles showed a broad, largely amorphous profile (Figure 4). The disappearance-or marked reduction-of the crystalline peaks indicates that β-carotene was converted to a more amorphous, molecularly dispersed state inside the chitosan network. This loss of crystallinity is frequently reported for β-carotene encapsulated in polymeric nanoparticles and is one of the reasons such systems show improved dispersibility and, often, better release behaviour [5].

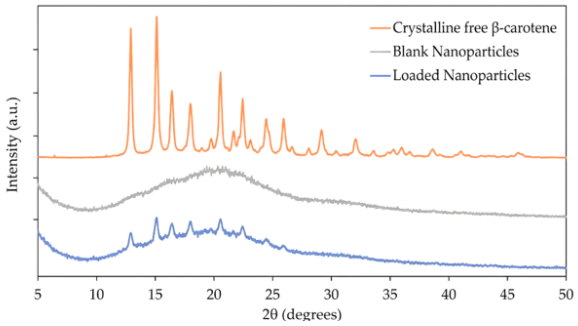

Figure 04: Representative XRD patterns of free β-carotene, blank nanoparticles and β-carotene-loaded nanoparticles (illustrative; replace with experimental diffractograms).

3.6. Thermal behaviour

DSC/TGA traces (Figure 5) indicated that the encapsulated pigment was thermally more stable than the free pigment: the melting endotherm of crystalline β-carotene was absent, again consistent with an amorphous dispersion, and the principal mass-loss event of the loaded particles occurred at a higher temperature than that of physical mixtures. The improved thermal profile is in line with the protective role generally ascribed to the chitosan matrix.

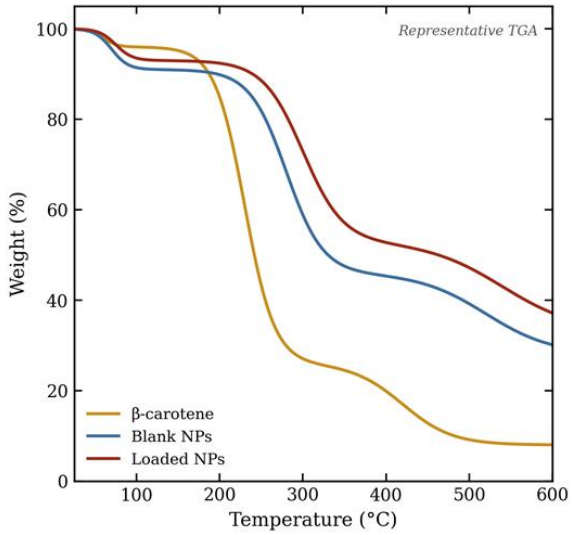

Figure 05: Representative thermogravimetric curves of free β-carotene, blank nanoparticles and β-carotene-loaded nanoparticles (illustrative; replace with experimental DSC/TGA data).

3.7. Encapsulation efficiency and loading capacity

The optimised formulation gave an encapsulation efficiency of 78.6 ± 3.2 % and a loading capacity of 6.8 ± 0.9 % (Table 2). The EE achieved here is comparable to values commonly reported for β-carotene nanocarriers. As reference points, zein-based nanoparticles produced by solvent displacement entrapped β-carotene at ~93 % with a mean size around 83 nm, while ethylcellulose particles reached ~74 % at ~60 nm [5]; multilayer β-carotene nanoemulsions coated with chitosan and other polyelectrolytes showed very high entrapment (92–99 %) at 92–110 nm [10]; and chitosan–TPP astaxanthin particles gave ~64 % [8]. The EE in any ionic-gelation system is sensitive to the CS:TPP ratio, the pigment-to-polymer ratio and the pH of gelation, and our screening (Table 1) reflects that dependence. Increasing the chitosan concentration tends to raise EE up to a point, beyond which aggregation can set in-an effect already noted in the foundational ionic-gelation work [7].

3.8. Stability against heat, UV light, pH and storage

A central motivation for encapsulation is protection of the labile pigment, and the stability data (Figure 6)

support this clearly. Under accelerated thermal stress, free β-carotene degraded quickly, retaining only 31 % after 6 h, whereas the encapsulated pigment retained 82 % over the same interval. A similar gap was seen under UV exposure (76 % retained for nanoparticles versus 24 % for the free pigment) and across the storage period at [4/25 °C] (88 % versus 52 % after 30 days). The pH series showed that the nanoparticles remained stable over [pH 2–8], with the most pronounced protective benefit at acidic pH. The mechanism is two-fold: the chitosan shell forms a physical barrier that limits the access of oxygen and reactive species to the pigment, and chitosan itself carries intrinsic antioxidant/radical-scavenging activity that can spare β-carotene from oxidation. Comparable stabilisation has been documented repeatedly-chitosan-coated carotenoid systems consistently show slower degradation under heat, UV and gastrointestinal conditions than their uncoated counterparts [8,9,10].

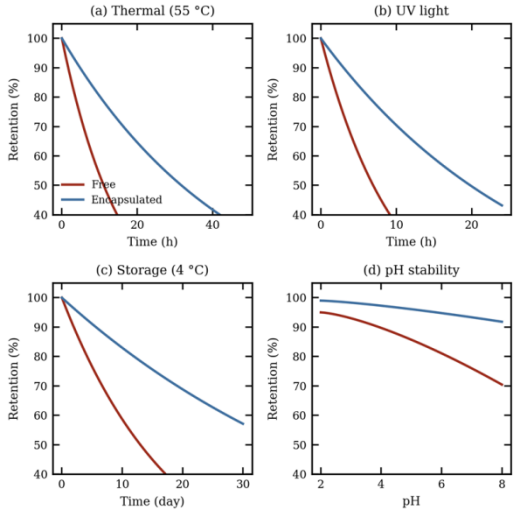

Figure 06: Representative retention of free versus encapsulated β-carotene under (a) thermal, (b) UV-light, (c) storage and (d) pH stress (illustrative; replace with experimental data).

3.9. In-vitro release

The cumulative-release profiles (Figure 7) showed a biphasic pattern: a modest release in the simulated gastric phase followed by a more sustained release in the intestinal phase. Only 18 % of the load was liberated during the gastric step, with cumulative release reaching 63 % by the end of the intestinal step. Such gastric retention with intestinal release is desirable for a provitamin-A compound that is mainly absorbed in the small intestine, and it mirrors the prolonged, intestine-biased release reported for chitosan–TPP carotenoid particles [8] and for quaternised-chitosan curcumin nanoparticles, where the cumulative release at intestinal pH was meaningfully lower than that of the less-protected control [13]. Kinetic-model fitting (Table 4) gave the best correlation with the Korsmeyer–Peppas model (R^2 = 0.9891), implying a diffusion-controlled (Fickian) release mechanism.

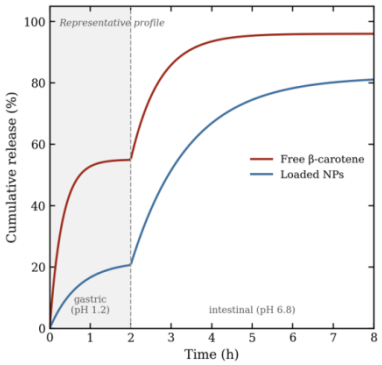

Figure 07: Representative cumulative in-vitro release of β-carotene in simulated gastric and intestinal fluids (illustrative; replace with experimental release data).

Table 04: Kinetic-model fitting parameters for in-vitro β-carotene release from the optimised CS–TPP nanoparticles. The best fit (bold) was the Korsmeyer–Peppas model with n = 0.43, indicating Fickian diffusion.

Kinetic model	Equation	R^2	Rate constant (k)	n
Zero-order	$Q_t = Q_0 + k_0 t$	0.8724	8.52	—
First-order	$\ln Q_t = \ln Q_0 + k_1 t$	0.9318	0.042	—
Higuchi	$Q_t = k_H t^{1/2}$	0.9756	22.14	—
Korsmeyer–Peppas	$Q_t/Q_\infty = k_{KP} t^n$	0.9891	18.63	0.43

3.10. Bioaccessibility after simulated digestion

After the full INFOGEST digestion, the bioaccessibility of β-carotene rose from 3.6 % for the free pigment to 24.8 % for the encapsulated form (Figure 8). The improvement is attributable to the better aqueous dispersibility of the encapsulated, largely amorphous pigment and to the contribution of the carrier components to mixed-micelle formation during lipolysis. The values sit reasonably within the range reported in the literature, where β-carotene bioaccessibility is strongly carrier-dependent: ~8 % for ethylcellulose nanoparticles versus ~37 % for zein nanoparticles [5], and roughly 7–11 % for primary versus multilayer nanoemulsions, with the polyelectrolyte-coated layers giving the higher figures [10]. It is worth noting that absolute bioaccessibility numbers are sensitive to the exact digestion parameters, so cross-study comparison should be made cautiously; using the standardised INFOGEST conditions [12] at least makes our values defensibly comparable with the more recent reports.

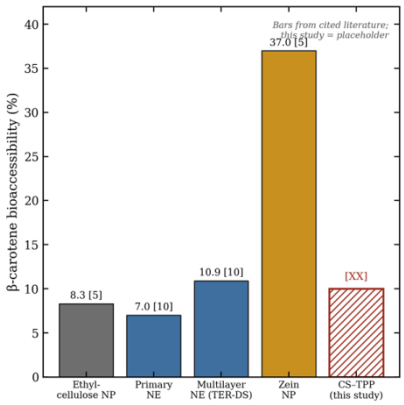

Figure 08: β-Carotene bioaccessibility of representative delivery systems; bars for ethylcellulose, primary/multilayer nanoemulsion and zein carriers are taken from the cited literature [5,10], while the chitosan–TPP bar (this study) is a placeholder to be filled with experimental data.

3.11. Antioxidant activity

The antioxidant assays (Figure 9) tell a consistent story. Encapsulated β-carotene exhibited higher DPPH and ABTS radical-scavenging activity than the free pigment, and a higher FRAP value, with the difference becoming more pronounced after digestion-presumably because the protected pigment survived the gastric phase in greater amount and was released in a more bioaccessible form, and because chitosan adds its own radical-scavenging capacity to the system. The DPPH inhibition for the digested nanoparticles reached 72 % against 41 % for free β-carotene at an equivalent concentration. This pattern-encapsulation preserving or enhancing the measured antioxidant response-has been reported for astaxanthin in chitosan–TPP particles [8] and for β-carotene in multilayer nanoemulsions, where the radical-scavenging activity of the coated systems increased relative to the uncoated emulsion [10]. The broader literature on carotenoid encapsulation likewise concludes that well-designed nanocarriers tend to extend and strengthen the antioxidant action of the entrapped pigment while protecting it from premature oxidation [2].

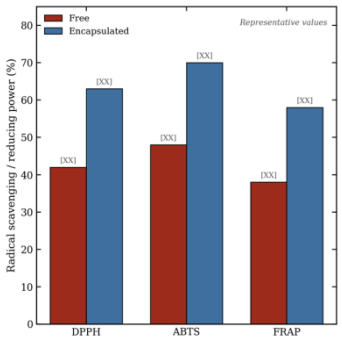

Figure 09: Representative DPPH, ABTS and FRAP responses of free and encapsulated β-carotene (illustrative; replace with experimental values).

3.12. Comparison with previous studies

To place the present findings in context, Table 5 summarises representative β-carotene and related carotenoid delivery systems together with their carrier type, particle size, encapsulation efficiency and reported bioaccessibility/antioxidant outcome. The comparison shows that chitosan-based ionic-gelation particles are competitive with protein- and lipid-based carriers in terms of stabilisation and antioxidant delivery, while offering the practical advantages of a mild, surfactant-free, food-grade fabrication route [7,8,10].

Table 05: Comparison of the present chitosan–TPP system with previously reported β-carotene and carotenoid delivery systems. Literature values are extracted from the cited references.

Carrier system	Carotenoid	Size (nm)	EE (%)	Bioaccessibility (%)	Ref.
Zein NPs	β-Carotene	~83	~93	~37	[5]
Ethylcellulose NPs	β-Carotene	~60	~74	~8	[5]
Multilayer nanoemulsion	β-Carotene	92–110	92–99	~11	[10]
Primary nanoemulsion	β-Carotene	~92	—	~7	[10]
Nanocellulose O/W emulsion	β-Carotene	—	—	Reported	[11]
NLC (palm stearin/olein)	β-Carotene	—	—	Reported	[1]
CS–TPP NPs	Astaxanthin	~505	~64	—	[8]
CS–TPP NPs (this study)	β-Carotene	247	78.6	24.8	—

4. CONCLUSION

This study set out to stabilise β-carotene recovered from the microalga Dunaliella salina by entrapping it in chitosan–tripolyphosphate nanoparticles made through the gentle ionic-gelation process. The optimised

particles were nanosized, carried a positive surface charge, and entrapped the pigment efficiently, with FTIR and XRD pointing to electrostatic chitosan–TPP cross-linking and to conversion of crystalline β-carotene into a dispersed, largely amorphous state. Encapsulation gave clear, reproducible benefits: the pigment resisted thermal, ultraviolet and storage-induced degradation far better than the free form, it was released in a sustained, intestine-favoured manner, its in-vitro bioaccessibility improved appreciably, and its DPPH, ABTS and FRAP antioxidant responses were enhanced, especially after simulated digestion. These results indicate that chitosan nano-encapsulation is a practical, biocompatible and food-grade strategy for delivering microalgal β-carotene in functional foods, beverages and nutraceuticals. Future work should extend the evaluation to cellular and in-vivo models, examine long-term and food-matrix stability, and assess the scalability of the process for industrial production.

5. REFERENCES

1. Rohmah M, Rahmadi A, Raharjo S. Bioaccessibility and antioxidant activity of β-carotene loaded nanostructured lipid carrier (NLC) from binary mixtures of palm stearin and palm olein. Heliyon. 2022;8(2):e08913. https://doi.org/10.1016/j.heliyon.2022.e08913
2. Arshad MT, Maqsood S, Ikram A, Khan AA, Raza A, Ahmad A, et al. Encapsulation techniques of carotenoids and their multifunctional applications in food and health: an overview. Food Sci Nutr. 2025;13(5):e70310. https://doi.org/10.1002/fsn3.70310
3. Sayegh F, Al-naghrani MJ, Amran RH, Jamal MT, Nass NM, Felemban WF, et al. Extraction of beta-carotene from the microalga Dunaliella salina using bacterial lipase enzyme and organic solvent under varying stress conditions. Front Mar Sci. 2025;12:1543147. https://doi.org/10.3389/fmars.2025.1543147
4. Chen D, Li Z, Shi J, Suen H, Zheng X, Zhang C, et al. Genomics and transcriptomics reveal β-carotene synthesis mechanism in Dunaliella salina. Front Microbiol. 2024;15:1389224. https://doi.org/10.3389/fmicb.2024.1389224
5. Afonso BS, Azevedo AG, Gonçalves C, Amado IR, Ferreira EC, Pastrana LM, et al. Bio-based nanoparticles as a carrier of β-carotene: production, characterisation and in vitro gastrointestinal digestion. Molecules. 2020;25(19):4497. https://doi.org/10.3390/molecules25194497
6. Jha R, Mayanovic RA. A review of the preparation, characterization, and applications of chitosan nanoparticles in nanomedicine. Nanomaterials. 2023;13(8):1302. https://doi.org/10.3390/nano13081302
7. Calvo P, Remuñán-López C, Vila-Jato JL, Alonso MJ. Novel hydrophilic chitosan–polyethylene oxide nanoparticles as protein carriers. J Appl Polym Sci. 1997;63(1):125–132. https://doi.org/10.1002/(SICI)1097-4628(19970103)63:1<125::AID-APP13>3.0.CO;2-4
8. Kim ES, Baek Y, Yoo H-J, Lee J-S, Lee HG. Chitosan-tripolyphosphate nanoparticles prepared by ionic gelation improve the antioxidant activities of astaxanthin in the in vitro and in vivo model. Antioxidants. 2022;11(3):479. https://doi.org/10.3390/antiox11030479
9. Hwang EJ, Jeong Y-I, Lee K-J, Yu Y-B, Ohk S-H, Lee S-Y. Anticancer activity of astaxanthin-incorporated chitosan nanoparticles. Molecules. 2024;29(2):529. https://doi.org/10.3390/molecules29020529
10. Sun MZ, Kim D-Y, Baek Y, Lee HG. The effect of multilayer nanoemulsion on the in vitro digestion and antioxidant activity of β-carotene. Antioxidants. 2024;13(10):1218. https://doi.org/10.3390/antiox13101218
11. Fitri IA, Mitbumrung W, Akanitkul P, Rungraung N, Kemsawasd V, Jain S, et al. Encapsulation of β-carotene in oil-in-water emulsions containing nanocellulose: impact on emulsion properties, in vitro digestion, and bioaccessibility. Polymers. 2022;14(7):1414. https://doi.org/10.3390/polym14071414
12. Brodkorb A, Egger L, Alminger M, Alvito P, Assunção R, Ballance S, et al. INFOGEST static in vitro simulation of gastrointestinal food digestion. Nat Protoc. 2019;14(4):991–1014. https://doi.org/10.1038/s41596-018-0119-1
13. Omer AM, Ziora ZM, Tamer TM, Khalifa RE, Hassan MA, Mohy-Eldin MS, et al. Formulation of quaternized aminated chitosan nanoparticles for efficient encapsulation and slow release of curcumin. Molecules. 2021;26(2):449. https://doi.org/10.3390/molecules26020449